CHALLENGES IN SIMULATING MW BEAMS IN CYCLOTRONS

Y. J. Bi *, Tsinghua University, Beijing, 100084, China & CIAE, Beijing, 102413, China &PSI
A. Adelmann †, R. Dölling, M. Humbel, W. Joho, M. Seidel, PSI, Villigen, CH-5234, Switzerland
T. J. Zhang, CIAE, Beijing, 102413, China; C. X. Tang, Tsinghua University, Beijing, 100084, China

Abstract

The 1.3 MW of beam power delivered by the PSI 590 MeV Ring Cyclotron together with stringent requirements regarding the controlled and uncontrolled beam losses poses great challenges with respect to predictive simulations. We describe a large scale simulation effort, which leads to a better quantitative understanding of the existing PSI high power proton cyclotron facility. Initial conditions for the PSI Ring simulations are obtained from a new time structure measurements and 18 profile monitors available in the 72 MeV injection line. The radial beam profile measurement which is just located in front of the extraction septum is compared with simulations. We show that OPAL (Object Oriented Parallel Accelerator Library) can precise predict the radial beam pattern at extraction with a large dynamic range of 4 orders of magnitude. A large turn separation and a narrow beam size at the Ring extraction is obtained by adjusting parameters such as the injection position and angle, the flattop phase and the trim coils. A large turn separation and a narrow beam size are the key elements for reducing the beam losses to acceptable levels. The described simulation capabilities are mandatory in the design and operation of the next generation high power proton drivers.

INTRODUCTION

A three stage proton accelerator complex is operated at the Paul Scherrer Institut. The 590 MeV Ring cyclotron, routinely delivers 2.2 mA of proton current, which makes it the most powerful machine of this kind worldwide. The resulting strong, phase-independent energy gain per revolution gives good turn separation and hence a beam extraction with low beam losses in the order of 10^{-4}. The upgrade plans of the PSI facility foresee a stepwise increase of the beam intensity to 3.0 mA [1].

Benefiting from the the High Performance Computing (HPC) clusters available today, the powerful tool OPAL enables us to perform large scale simulations in complex high intensity accelerators [2]. OPAL is a tool for charged-particle optic calculations in accelerator structures and beam lines including 3D space charge. A new particle matter interaction model taking into account energy loss, multiple Coulomb scattering and large angle Rutherford scattering is now available. This model together with the 3D space charge will significantly increase the predictive capabilities of OPAL.

* biyj05@mails.tsinghua.edu.cn
† andreas.adelmann@psi.ch

THE PHYSICAL MODEL

To perform large scale simulations in complex high intensity cyclotrons, both space charge effect and the particle matter interaction should be considered carefully. The original version of OPAL can deal with not only single bunch space charge effects but also the effects of neighboring bunches [3], however, the particle matter interaction is missing. General-purpose Monte Carlo codes, e.g. MCNPX [4], FLUKA [5, 6], are developed to model the particle matter interaction, however they have limited capabilities to track the particle in both complex external and space charge fields. We extend OPAL in order to handle efficient particle matter interactions, hence collimator systems in high intensity accelerators can be modeled together with space charge.

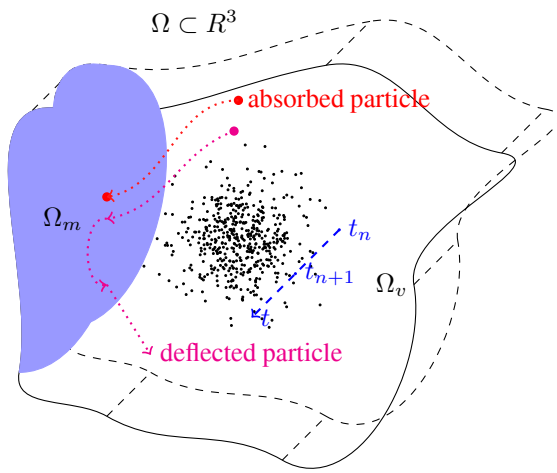

Figure 1: The beam and its surrounding region.

The Fig.1 describes the computational domain Ω surrounding the beam. It is divided into two sub-domains: the vacuum domain Ω_v and the material domain Ω_m. When the beam is passing collimator or in general 'material', some of the halo particle maybe go from the vacuum domain into the material domain. This part of the beam is then absorbed or deflected.

The flowchart with physical model in material is shown in Fig. 2. If the coordinate of a particle is in the material region, $x \in \Omega_m$, a temporal sub-stepsize is defined as

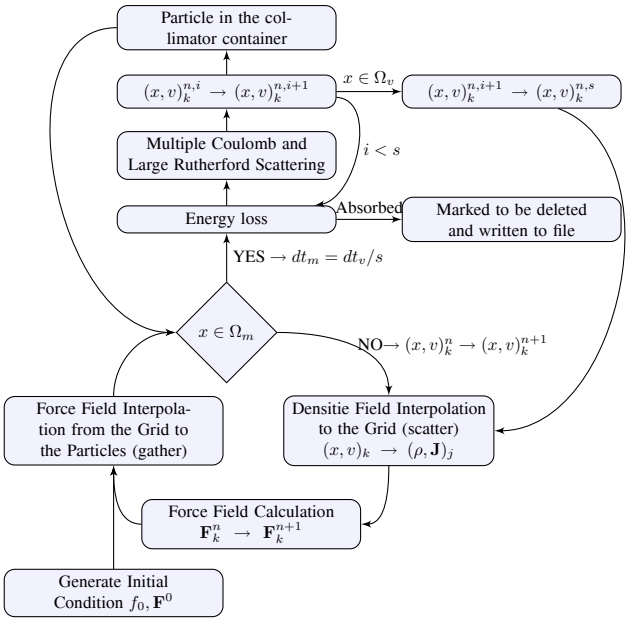

Figure 2: The flowchart with physical model in material.

$dt_m = dt_v/s$, where dt_v is the stepsize in vacuum and s is an integer. When the particle interacts with the matter, the energy loss is calculated using the Bethe-Bloch equation. Comparing the stopping power with the PSTAR program of National Institute of Standards and Technology (NIST), the error is found in the order of 10% for copper, from several MeV to 10 GeV. For applications at PSI, the error is within 3% in the region from 50 MeV to 1 GeV. In general, there is energy straggling when a beam passes through the material. For relatively thick absorbers, when the number of collisions is large, the energy loss distribution is Gaussian [7]. If the energy of the particle is low enough to be absorbed after a certain distance, it is marked to be deleted and is written to a file. The Coulomb scattering is treated as two independent events: the multiple Coulomb scattering and the large angle Rutherford scattering, using the distribution given in [8]. After applying these physics processes, the particles are pushed one sub-step $(x,v)_k^{n,i} \rightarrow (x,v)_k^{n,i+1}$. If the particles coming back to the vacuum domain, another $(s-i)$ sub-steps $(x,v)_k^{n,i+1} \rightarrow (x,v)_k^{n,s}$ are applied, treating the particles motion as in a drift space. Otherwise, the loop goes on until s sub-steps finish and then the particles are stored in the collimator container.

As a benchmark of the collimator models in OPAL, the energy spectrum and angle deviation is compared against two general-purpose Monte Carlo codes, MCNPX and FLUKA, as shown in Fig. 3. A 72 MeV cold Gaussian beam with $\sigma_x = \sigma_y = 5$ mm is send through a elliptic copper collimator with the half aperture of 3 mm in both x and y direction from 0.01 m to 0.1 m. The deflected particles contribute to the energy spectrum and angle deviation after a collimator. These particles may be lost downstream. A very good agreement of our model w.r.t. MCNPX and FLUKA is shown in Fig. 3.

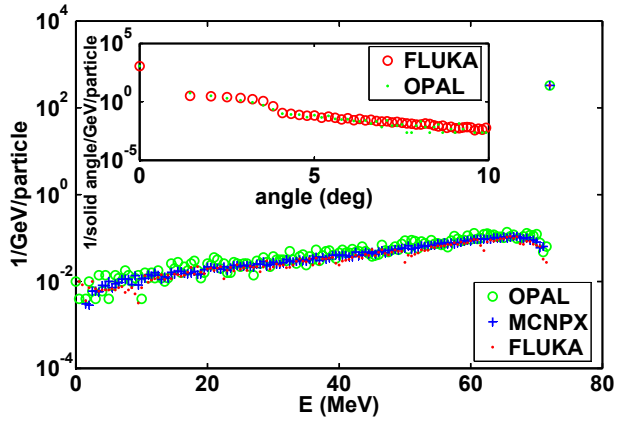

Figure 3: Energy spectrum and angle deviation (small plot).

OBTAINING INITIAL CONDITIONS FOR THE RING CYCLOTRON

The simulation starts at the beginning of the 72 MeV transfer line between the Inj. 2 and Ring cyclotron. There are 18 beam profile monitors in both x and y direction at the transfer line. The initial distribution is obtained using transport [9] by fitting the profile monitor data. We obtain the non-normalized rms emittance $\epsilon_x = 2.25\ \pi\ mm\ mrad$, $\epsilon_y = 0.5\ \pi\ mm\ mrad$. The rms moment spread is 0.1%. Fig. 4 shows the comparison of the envelope between OPAL-T and the measurement. Before the bending

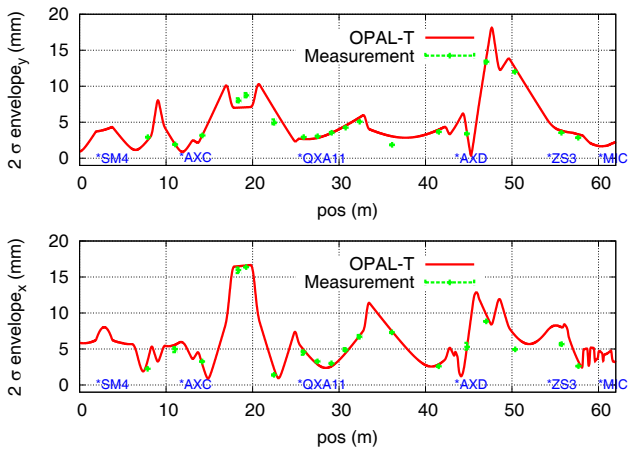

Figure 4: Envelope of the beam at the 72 MeV transfer line for 2 mA beam.

magnet MIC, the agreement between OPAL-T , transport and measurement is very well. After MIC, it is already the start of the Ring cyclotron. At the position of MIC, we switch from OPAL-T to OPAL-CYCL which is developed as a general purpose cyclotron tracker.

For the start of the Ring simulation, the emittance acquired at the end of the transfer line is used. The length of the bunch is measured using the time-structure probes [10].

Different distributions such as a six-dimensional Gaussian or parabolic are used for the Ring cyclotron simulations. For a 2 mA beam we obtained the non-normalized radial emittance as 1.5 π mm $mrad$, the vertical emittance is 0.6 π mm $mrad$, and the standard deviation of bunch length is $\sigma = 23$ mm.

TOWARDS REALISTIC SIMULATIONS IN THE RING CYCLOTRON

Beam losses during the operation of the cyclotron usually limits the intensity that can be extracted. The PSI 590 MeV Ring which routinely delivers 2.2 mA beam has a very low loss rate in the order of 0.02% to avoid excessive activation of accelerator components and keep the radiation dose imposed on the personnel involved in maintenance at acceptable levels. Therefore, the understanding of the beam dynamics, most important in the extraction region, is one of the key points to be addressed if power levels increase.

The Flattop Phase

Although a compact beam is observed in the extraction of the Inj. 2 cyclotron, the bunch length increases to about $\sigma = 23$ mm at injection into the Ring after passing through the almost 60 m long (72 MeV) transfer line. For such a long "pencil" beam, a flattop cavity is needed to compensate the energy difference from the main cavity and also avoid the formation of the S-shape beam caused by space charge effects.

When there is no space charge effect, the ideal flattop makes the total energy gain of any particle almost the same independent of the RF phase. Considering a high current beam, the flattop phase should be shifted to make the tail particle gains more energy than the head one to compensate the linear part of the space charge force. The phase of the flattop is intensity-dependent, therefore there exists an optimum flattop phase for an given intensity.

The Effect of the Trim Coil TC15

In the original design of the Ring cyclotron, the beam will pass the coupling resonance $\nu_r = 2\nu_z$ four times at 490, 525, 535 and 585 MeV. A large horizontal oscillation is transformed into a large vertical one at the coupling resonance which can lead to vertical beam losses. A trim coil TC15 is designed to avoid the resonance at 525 and 535 MeV [11]. It provides an additional magnet field and field gradient in the radial direction as shown in Fig. 5. The trim coil provides a maximum magnetic field of 14 Gs. It has a long tail towards the smaller radii in order to make the integrated strength of the trim coil over the radius to zero.

The radial and vertical tune shift caused by TC15 is,

$$\begin{cases} \Delta\nu_r \approx \frac{R}{2\nu_r B}\frac{d\overline{B}}{dR} \approx 0.014 \\ \Delta\nu_z \approx -\frac{\nu_r}{\nu_z}\Delta\nu_r \approx -2\Delta\nu_r \approx -0.028 \end{cases} \quad (1)$$

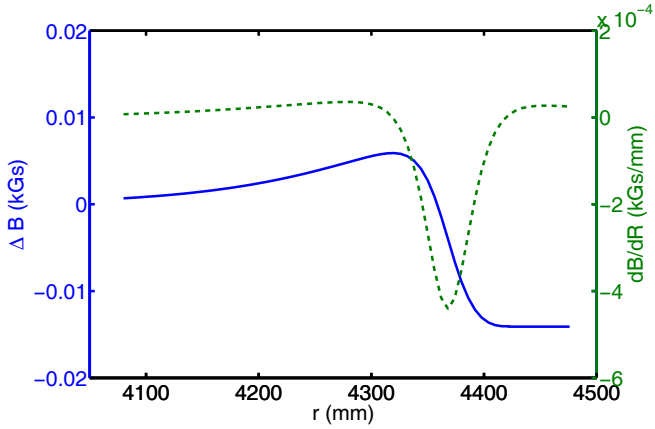

Figure 5: Additional field provided by TC15.

where R is the orbit radius, B is the hill field, $\frac{d\overline{B}}{dR}$ is the average field gradient in radial direction.

Fig. 6 shows the tune diagram with and without TC15.

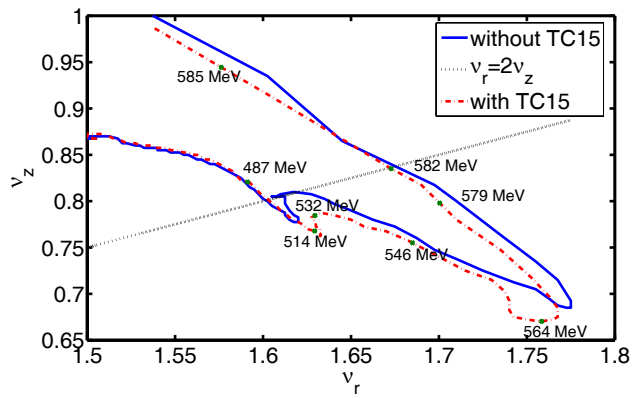

Figure 6: Tune diagram with and without TC15.

The Injection Position and Angle

It is important to make the radial beam size at the extraction region smaller than the turn separation in order to be able to extract the beam in a single turn. The turn separation for a centered beam is defined as

$$\frac{dR}{dn} = \frac{\gamma}{\gamma+1} R \frac{dE/dn}{E} \frac{1}{1+n}, \quad (2)$$

where n is the field index. It it only about 6.0 mm at the extraction region of the Ring cyclotron. To get large turn separation, a non-centered injection into the Ring cyclotron is used. Since $\nu_r \approx 1.7$ in the extraction region, adjusting the injection position and angle, results in the betatron amplitude being almost equal to the radius gain per turn. The formation of the turn pattern for the last four turn is shown in Fig. 7. This is a special turn pattern because the last turn is well separated from the overlapping second, third and fourth last turns. In this case, the turn separation at the

extraction turn is as large as 16 mm, hence it allows the extraction of high intensity beam with very low losses.

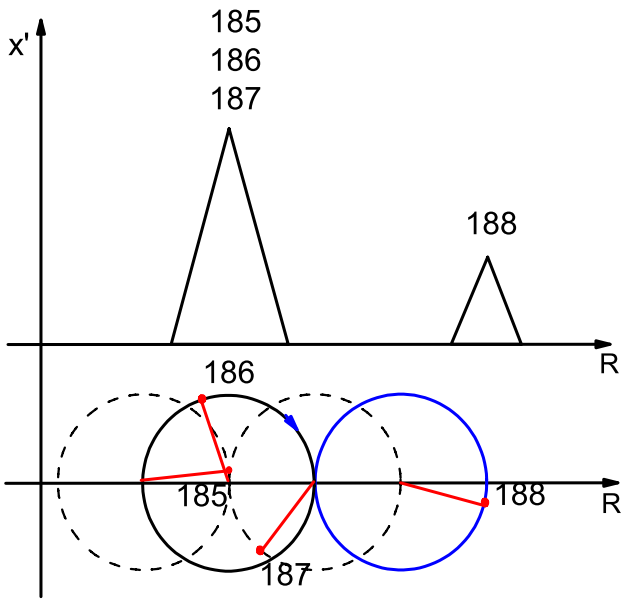

Figure 7: Formation of the turnpattern in PSI Ring cyclotron.

The Radial Profile at Probe RRE4

To compare the above analysis with measurements, a radial probe is implemented in OPAL-CYCL. In the 590 MeV Ring at PSI, the radial probe RRE4 located just before the extraction septum. This probe is able to record the radial profile of the last nine turns. The measurement as well as the simulations are carried out at 2 mA. The flattop phase and the injection position and angle is optimized to get the largest turn separation and smallest beam size at the extraction region. The effect of the trim coil TC15 on the turn pattern is shown in Fig. 8. For fixed energy, it brings a shift of orbit center by $\frac{\Delta R}{R} = -\frac{\Delta B}{B}$. In our case, $\Delta R\mid_{max} \approx 3mm$, hence the center of turn 180 moves to the exact position of the measurement when considering the effect of the TC15. Figure 8 also shows that the valley at the position of septum gets closer to the measurement if the initial distribution is supposed to be parabolic. It is because the gaussian distribution has a long tail which can contribute to the minimum value.

CONCLUSIONS AND DISCUSSIONS

In this paper, we present novel simulations for the beam dynamics in high intensity cyclotrons. For the first time we are able to obtain a realistic understanding of the beam dynamics in the very complex PSI Ring cyclotron by means of 3D particle simulations.

By a proper consideration of the initial distribution, according to measurements of beam profile monitors, and the

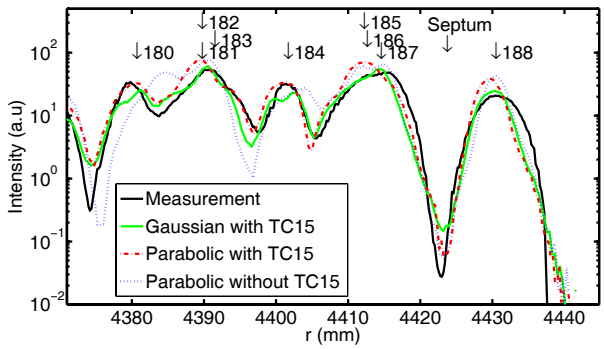

Figure 8: Radial beam profile with indicated turn numbers at extraction for 2 mA beam.

time structure of the beam, realistic simulations of the PSI Ring cyclotron are presented and compared to measurements. Very good agreement for the radial probe between the simulation and measured data is obtained by adjusting the injection position, angle, flattop voltage, phase, and the trim coil TC15. These parameter are all in agreement with settings obtained from the control room.

Particle matter interaction is included in OPAL to track particles with off-momenta and angles in both external and space charge fields. This enables the prediction of lost particles including space charge which can't be done with general-purpose Monte Carlo codes.

The presented results can be extrapolated to other accelerators and enable the precise prediction of crucial parameters, such as losses, in next generation high power cyclotrons.

ACKNOWLEDGMENTS

The authors thank the Accelerator Modeling and Advanced Computing group members C. Kraus, Y. Ineichen and J. J. Yang for many discussions regarding programming and T. Schietinger for providing the post-processing tool H5PartRoot. We also thank D. Kiselev for the MCNPX simulations and fruitful discussions w.r.t. the particle matter interaction models, and H. Zhang for providing the element information in the 72 MeV line and the Ring cyclotron. This work was partly performed on the *felsim* cluster at the Paul Scherrer Institut and on the Cray XT5 at Swiss National Supercomputing Center (CSCS) within the "Horizon" collaboration.

REFERENCES

[1] M.Seidel et al, Production of a 1.3 MW Proton Beam at PSI, IPAC10, p.1309, Kyoto (2010).

[2] A. Adelmann, Ch. Kraus, Y. Ineichen et al., The Object Oriented Parallel Accelerator Library (OPAL), Design, Implementation and Application, Proceedings of ICAP'09, (2009).

[3] J. J. Yang, A. Adelmann, M. Humbel, et al., Beam Dynamics in High Intensity Cyclotrons Including Neighbor-

ing Bunch Effects: Model, Implementation and Application. Phys. Rev. ST Accel. Beams 13, 064201, (2010).

[4] D. Pelowitz ed., MCNPX User's Manual, Version 2.5.0 LA-CP-05-0369, (2005).

[5] G. Battistoni, S. Muraro, P.R. Sala, F. Cerutti, A. Ferrari, S. Roesler, A. Fasso', J. Ranft, The FLUKA code: Description and benchmarking, roceedings of the Hadronic Shower Simulation Workshop 2006, Fermilab 6–8 September 2006, M. Albrow, R. Raja eds., AIP Conference Proceeding 896, 31-49, (2007).

[6] A. Fasso, A. Ferrari, J. Ranft, and P.R. Sala, FLUKA: a multi-particle transport code, CERN-2005-10 (2005), INFN/TC_05/11, SLAC-R-773.

[7] William R. Leo, Techniques for nuclear and particle physics experiments, 2nd, Springer-Verlag, Berlin Heidelberg New York, (1994).

[8] J. D. Jackson, Classical Electrodynamics, 3rd, John Wiley &. Sons, New York, (1998).

[9] U. Rohrer, PSI Graphic Transport Framework based on a CERN-SLAC-FERMILAB version by K.L. Brown et al. (2007).

[10] R. Döling, New time-structure probes between injector and Ring cyclotron, PSI - Scientific and Technical Report 2004 / Volume VI, (2004).

[11] S. Adam and W. Joho, Tech. Report, TM-11-13, (1974).